

# C–H Activation and Functionalization of Unsaturated Hydrocarbons by Transition-Metal Boryl Complexes

Karen M. Waltz, Clare N. Muhoro, and John F. Hartwig\*

Department of Chemistry, Yale University, P.O. Box 208107,  
New Haven, Connecticut 06520-8107

Received February 19, 1999

Transition-metal boryl complexes of the form  $\text{Cp}'\text{Fe}(\text{CO})\text{LBcat}$  and  $(\text{CO})_5\text{MBcat}$ , where  $\text{Cp}' = \text{C}_5\text{H}_5$ ,  $\text{C}_5\text{Me}_5$ ,  $\text{M} = \text{Mn}$ ,  $\text{Re}$ ,  $\text{L} = \text{CO}$ ,  $\text{PMe}_3$ , and  $\text{cat} = 1,2\text{-O}_2\text{C}_6\text{H}_4$ , were synthesized by reaction of  $\text{ClBcat}$  with  $[\text{Cp}'\text{Fe}(\text{CO})\text{L}]^-$  or  $[\text{M}(\text{CO})_5]^-$ . X-ray crystal structures of  $\text{CpFe}(\text{CO})_2\text{Bcat}$ ,  $\text{Cp}^*\text{Fe}(\text{CO})_2\text{Bcat}$ , and  $(\text{CO})_5\text{MnBcat}$  were obtained. Upon irradiation, these metal boryl complexes reacted with arenes and alkenes to form aryl- and vinylboronate ester products in moderate to high yields. Monosubstituted arenes with methyl, chloro, trifluoromethyl, methoxy, and dimethylamino substituents were used as substrates, and the resulting ratios of ortho- to meta- to para-substituted arene products were measured. No significant electronic effects were observed, indicating that the chemistry is not occurring through a typical electrophilic aromatic substitution pathway. Competition experiments between toluene and other substituted arenes were conducted. Reactivity differences were small, but anisole was found to have the fastest rate of reaction. Kinetic isotope effects were measured for the reaction of  $\text{CpFe}(\text{CO})_2\text{Bcat}$ ,  $(\text{CO})_5\text{MnBcat}$ , or  $(\text{CO})_5\text{ReBcat}$  with benzene/benzene- $d_6$  mixtures and were found to be  $3.3 \pm 0.4$ ,  $2.1 \pm 0.1$ , and  $5.4 \pm 0.4$ , respectively. This difference in isotope effect along with differences in selectivities with substituted arsenic reagents rules out a mechanism by which a common free Bcat radical attacks free substrate. Several experiments were also conducted to probe for CO loss. A  $^{13}\text{C}$ -labeling experiment, CO inhibition experiment, and  $\text{PMe}_3$  trapping experiment indicate that the mechanism most likely proceeds through irreversible CO loss to form a 16-electron intermediate. Functionalization of alkenes to form vinylboronate esters was also observed, and mechanistic studies showed the absence of a measurable kinetic isotope effect for reaction of  $\text{CpFe}(\text{CO})_2\text{Bcat}$  or  $(\text{CO})_5\text{ReBcat}$  with ethylene/ethylene- $d_4$  mixtures or for reaction with ethylene- $d_2$ .

## Introduction

The functionalization of unreactive C–H bonds has been a major goal of organometallic chemistry.<sup>1–3</sup> Many homogeneous organometallic systems undergo intermolecular C–H activation reactions with unsaturated as well as saturated organic substrates, but few lead to unbound functionalized products.<sup>3</sup> Of the systems that cleave hydrocarbon C–H bonds, many contain an aromatic supporting ligand such as cyclopentadienide. For example, unsaturated metal fragments of the form  $\text{CpIrL}_x$  were shown in the early 1980s to react with hydrocarbons to form isolable metal alkyl hydride complexes, providing some of the first evidence for oxidative addition of alkane C–H bonds.<sup>4–6</sup> In contrast, no metal carbonyl fragments of the form  $\text{M}(\text{CO})_x\text{R}$  or even  $\text{CpM}(\text{CO})_2\text{R}$  ( $\text{M} = \text{Fe}$ ,  $\text{Ru}$ ,  $\text{Os}$ ) have been reported to react with free arene or alkane C–H bonds to date. Future studies may reveal such reactivity.

Thus, systems that can selectively deliver a functional group to a hydrocarbon are current targets. Some examples of functionalization processes mediated by homogeneous transition-metal systems include dehydrogenation of alkanes,<sup>7–9</sup> carbonylation of benzene,<sup>10–12</sup> carbonylation of pentane,<sup>13</sup> and aldimine formation from isonitrile insertion into benzene.<sup>14</sup> Recently, oxidation of hydrocarbons by electrophilic late transition metals<sup>15</sup> has shown renewed promise.<sup>16</sup> A Pt system developed recently by Periana et al. selectively catalyzes the conversion of methane to methyl bisulfate in 70% yield at temperatures as low as 100 °C.<sup>17</sup> This method of

(1) Arndtsen, B. A.; Bergman, R. G.; Mobley, T. A.; Peterson, T. H. *Acc. Chem. Res.* **1995**, *28*, 154–162.

(2) Crabtree, R. H. *Chem. Rev.* **1985**, *85*, 245–269.

(3) *Activation and Functionalization of Alkanes*; Hill, C. L., Ed.; Wiley: New York, 1989.

(4) Hoyano, J. K.; McMaster, A. D.; Graham, W. A. G. *J. Am. Chem. Soc.* **1983**, *105*, 7190–7191.

(5) Janowicz, A. H.; Bergman, R. G. *J. Am. Chem. Soc.* **1983**, *105*, 3929–3939.

(6) Jones, W. D.; Feher, F. J. *Organometallics* **1983**, *2*, 562–563.

(7) Burk, M. J.; Crabtree, R. H. *J. Am. Chem. Soc.* **1987**, *109*, 8025–8032.

(8) Maguire, J. A.; Boese, W. T.; Goldman, A. S. *J. Am. Chem. Soc.* **1989**, *111*, 7088–7093.

(9) Maguire, J. A.; Goldman, A. S. *J. Am. Chem. Soc.* **1991**, *113*, 6706–6708.

(10) Kunin, A. J.; Eisenberg, R. *J. Am. Chem. Soc.* **1986**, *108*, 535–536.

(11) Kunin, A. J.; Eisenberg, R. *Organometallics* **1988**, *7*, 2124–2129.

(12) Fisher, B. J.; Eisenberg, R. *Organometallics* **1983**, *2*, 764–767.

(13) Sakakura, T.; Tanaka, M. *J. Chem. Soc., Chem. Commun.* **1987**, 758–759.

(14) Jones, W. D.; Foster, G. P.; Putinas, J. M. *J. Am. Chem. Soc.* **1987**, *109*, 5047–5048.

(15) Shilov, A. E.; Shul'pin, G. B. *Chem. Rev.* **1997**, *97*, 2879.

(16) Stahl, S. S.; Labinger, J. A.; Bercaw, J. E. *Angew. Chem., Int. Ed.* **1998**, *37*, 2180–2192.

generating an ester of methanol eliminates the common problem of higher reactivity of the product and over-oxidation. A recent iridium complex with a PCP-type ligand leads to acceptorless dehydrogenation of cyclic alkanes or transfer dehydrogenation of linear alkanes to form  $\alpha$ -olefins as the predominant product at early reaction times.<sup>18</sup> More traditional methods to functionalize hydrocarbons are based on radical or superacidic reagents. However, these reagents react with poor selectivity for different types of C–H bonds. Even enzymatic systems or models of them usually show poor selectivity upon oxidation of linear alkanes.<sup>19</sup> Homogeneous transition-metal systems should be able to overcome this selectivity problem because they react preferentially with primary C–H bonds.

We have found that the presence of a boryl ligand in the  $M(\text{CO})_x$  and  $\text{Cp}M(\text{CO})_2$  ( $M = \text{Fe}, \text{Ru}$ ) metal systems that previously showed no intermolecular C–H activation creates a system that is reactive not only toward the cleavage of hydrocarbon C–H bonds but also toward elimination of functionalized organoboronate ester products. We have previously communicated the functionalization of arenes and alkenes by  $\text{CpFe}(\text{CO})_2\text{Bcat}$  and  $(\text{CO})_5\text{MBcat}$  ( $M = \text{Mn}, \text{Re}$ )<sup>20</sup> to form aryl- and vinylboronate esters. This functionalization chemistry is unusual for organometallic systems, and the initial C–H bond cleavage must result from the presence of the boryl group.

The boryl group's effect on the reactivity and regiochemistry for HX bonds was initially demonstrated by the reactions of metal boryl complexes with protic reagents.<sup>21</sup> In these transformations, a metal hydride was formed and an aminoborane, alkoxoborane, or haloborane was formed from reaction with an amine, alcohol, or mineral acid. Reaction with hydrocarbons occurs with similar regiochemistry to produce a metal hydride and a hydrocarbon with a boryl functional group. The boryl ligand's dramatic effect on the reactivity of the metal center may be due to its electrophilic strong  $\sigma$ -donating ability of the anionic boryl ligand. Alternatively, functionalization of hydrocarbons with boryl complexes may result from the thermodynamic driving force provided by formation of strong boron–carbon bonds.<sup>22,23</sup> We report here a full synthetic and mechanistic account of the functionalization of arenes and alkenes by transition-metal boryl complexes to form aryl- and vinylboronate esters. These organoboronate ester compounds are useful organic intermediates that can be converted into a variety of functionalized organic molecules, such as alcohols, amines, aldehydes, and halides.<sup>24–26</sup>

(17) Periana, R. A.; Taube, D. J.; Gamble, S.; Taube, H.; Satoh, T.; Fujii, H. *Science* **1998**, *280*, 560–564.

(18) Liu, F.; Pak, E. B.; Singh, B.; Jensen, C. M.; Goldman, A. S. *J. Am. Chem. Soc.* **1999**, *121*, 4086–4087.

(19) Cook, B. R.; Reinert, T. J.; Suslick, K. S. *J. Am. Chem. Soc.* **1986**, *108*, 7281–7286.

(20) Waltz, K. M.; He, X.; Muhoro, C.; Hartwig, J. F. *J. Am. Chem. Soc.* **1995**, *117*, 11357–11358.

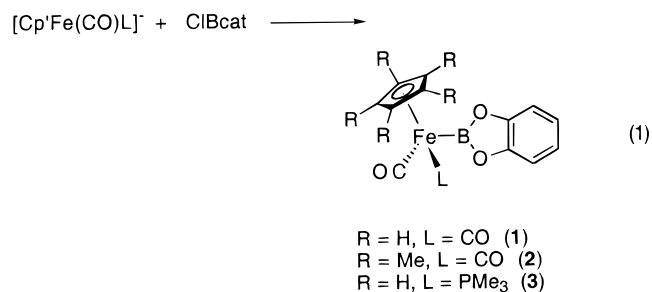
(21) Hartwig, J. F.; Huber, S. *J. Am. Chem. Soc.* **1993**, *115*, 4908–4909.

(22) Rablen, P. R.; Hartwig, J. F.; Nolan, S. P. *J. Am. Chem. Soc.* **1994**, *116*, 4121.

(23) Rablen, P. R.; Hartwig, J. F. *J. Am. Chem. Soc.* **1996**, *118*, 4648–4653.

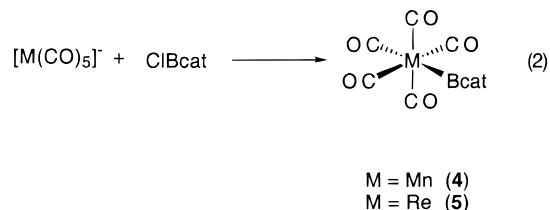
## Results

**A. Synthesis and Characterization of Transition-Metal Boryl Complexes.** Transition-metal boryl complexes of the general formula  $\text{Cp}'\text{Fe}(\text{CO})\text{LBcat}$  ( $\text{Cp}' = \text{C}_5\text{H}_5, \text{C}_5\text{Me}_5$ ;  $\text{L} = \text{CO}, \text{PMe}_3$ ;  $\text{cat} = 1,2\text{-O}_2\text{C}_6\text{H}_4$ ) were prepared by addition of  $\text{ClBcat}$  to a suspension of  $M[\text{Cp}'\text{Fe}(\text{CO})\text{L}]$  ( $M = \text{Na}, \text{Li}$ ) in toluene solvent as shown in eq 1. With the exception of  $\text{Li}[\text{Cp}'\text{Fe}(\text{CO})\text{L}]$ ,



( $\text{PMe}_3$ ), all metal anions used in the syntheses of the metal boryl complexes were prepared by  $\text{Na}/\text{Hg}$  reduction of the corresponding metal dimers in THF. The reactions were monitored by  $^{11}\text{B}$  NMR spectroscopy, which showed the disappearance of  $\text{ClBcat}$  at  $\delta$  29, and the formation of a new peak between  $\delta$  44 and 57 corresponding to the  $\text{Cp}'\text{Fe}(\text{CO})\text{LBcat}$  complex. In the case of the parent  $\text{CpFe}(\text{CO})_2\text{Bcat}$  complex (**1**), a saturated pentane solution of the crude product was crystallized at  $-30$  °C for 20–30 min to give a 73% yield of yellow product. Yellow  $\text{Cp}^*\text{Fe}(\text{CO})_2\text{Bcat}$  (**2**) was isolated in 71% yield from  $\text{Na}[\text{Cp}^*\text{Fe}(\text{CO})_2]$ , and  $\text{CpFe}(\text{CO})(\text{PMe}_3)\text{Bcat}$  (**3**) was isolated in 33% yield from  $\text{Li}[\text{CpFe}(\text{CO})(\text{PMe}_3)]$  (**4**) prepared by deprotonation of the known  $\text{CpFe}(\text{CO})(\text{PMe}_3)\text{H}$ <sup>27</sup> with  $n\text{-BuLi}$ . The bis(phosphine) complex  $\text{CpFe}(\text{PMe}_3)_2\text{Bcat}$  (**5**) was synthesized by irradiation of **1** in excess  $\text{PMe}_3$  in pentane. Recrystallization from toluene removed traces of  $\text{CpFe}(\text{CO})(\text{PMe}_3)\text{Bcat}$  impurity and gave **5** in 52% yield.

The metal boryl complexes  $(\text{CO})_5\text{MBcat}$  ( $M = \text{Mn}$  (**6**),  $\text{Re}$  (**7**)) were prepared in a similar fashion by addition of  $\text{ClBcat}$  to a suspension of  $\text{Na}[M(\text{CO})_5]$  in toluene (eq 2). These reactions were also monitored by  $^{11}\text{B}$  NMR



spectroscopy, which showed new peaks for **6** and **7** at  $\delta$  49 and 44. Crystallization from toluene layered with pentane afforded **6** and **7** in 72% and 30% yields, respectively.

(24) Brown, H. C. *Boranes in Organic Chemistry*; Cornell University Press: Ithaca, NY, 1972.

(25) Brown, H. C. *Organic Synthesis via Boranes*; Wiley: New York, 1975.

(26) Pelter, A.; Smith, K.; Brown, H. C. *Borane Reagents*; Academic Press: New York, 1988.

(27) Treichel, P. M.; Komar, D. A. *J. Organomet. Chem.* **1981**, *206*, 77–88.

**Table 1. Crystallographic Data for CpFe(CO)<sub>2</sub>Bcat (1), Cp\*Fe(CO)<sub>2</sub>Bcat (2), and (CO)<sub>5</sub>MnBcat (6)**

	CpFe(CO) <sub>2</sub> Bcat	Cp*Fe(CO) <sub>2</sub> Bcat	(CO) <sub>5</sub> MnBcat
empirical formula	C <sub>13</sub> H <sub>9</sub> O <sub>4</sub> BFe	C <sub>18</sub> H <sub>19</sub> O <sub>4</sub> BFe	C <sub>11</sub> H <sub>4</sub> O <sub>7</sub> BMn
fw	295.87	366.00	313.90
cryst color, habit	pale yellow parallelogram	pale yellow prism	golden yellow cut block
cryst dimens (mm)	0.20 × 0.20 × 0.45	0.19 × 0.29 × 0.46	0.35 × 0.35 × 0.42
cryst syst	orthorhombic	monoclinic	monoclinic
space group	<i>P</i> 2 <sub>1</sub> 2 <sub>1</sub> 2 <sub>1</sub> (No. 19)	<i>P</i> 2 <sub>1</sub> / <i>a</i> (No. 14)	<i>P</i> 2 <sub>1</sub> / <i>a</i> (No. 14)
temp (K)	296	183	296
lattice params			
<i>a</i> (Å)	9.5178(6)	8.016(1)	12.865(9)
<i>b</i> (Å)	9.608(1)	24.49(1)	7.019(6)
<i>c</i> (Å)	13.713(2)	8.737(1)	15.296(4)
$\beta$ (deg)		96.06(2)	113.17(2)
<i>V</i> (Å <sup>3</sup> )	1254.0(4)	1706(1)	1270(2)
<i>Z</i>	4	4	4
<i>D</i> <sub>calcd</sub> (g/cm <sup>3</sup> )	1.567	1.425	1.642
residuals			
<i>R</i>	0.030	0.034	0.038
<i>R</i> <sub>w</sub>	0.032	0.043	0.040
goodness of fit indicator	1.27	2.55	2.24

**Table 2. Selected Bond Distances for CpFe(CO)<sub>2</sub>Bcat (1) and Cp\*Fe(CO)<sub>2</sub>Bcat (2)<sup>a</sup>**

	CpFe(CO) <sub>2</sub> Bcat	Cp*Fe(CO) <sub>2</sub> Bcat
Fe–B	1.959(6)	1.980(2)
Fe–C7	1.734(5)	1.749(3)
Fe–C8	1.728(6)	1.743(2)
Fe–Cp' centroid	1.7155(7)	1.72(1)
B–O1	1.401(6)	1.404(3)
B–O2	1.420(7)	1.410(3)

<sup>a</sup> Distances are in angstroms. Estimated standard deviations in the least significant figure are given in parentheses.

**Table 3. Selected Bond Angles for CpFe(CO)<sub>2</sub>Bcat (1) and Cp\*Fe(CO)<sub>2</sub>Bcat (2)<sup>a</sup>**

	CpFe(CO) <sub>2</sub> Bcat	Cp*Fe(CO) <sub>2</sub> Bcat
C7–Fe–C8	92.9(3)	96.3(1)
C7–Fe–B	83.5(3)	87.5(1)
C8–Fe–B	87.1(2)	82.82(9)
Fe–B–O1	127.0(4)	126.8(2)
Fe–B–O2	125.0(4)	124.4(2)
O1–B–O2	108.0(5)	108.8(2)

<sup>a</sup> Angles are in degrees. Estimated standard deviations in the least significant figure are given in parentheses.

**Table 4. Selected Bond Distances for (CO)<sub>5</sub>MnBcat (6)<sup>a</sup>**

	(CO) <sub>5</sub> MnBcat	(CO) <sub>5</sub> MnBcat	(CO) <sub>5</sub> MnBcat
Mn–B	2.108(6)	Mn–C10	1.847(7)
Mn–C7	1.870(7)	Mn–C11	1.832(8)
Mn–C8	1.841(6)	B–O1	1.373(6)
Mn–C9	1.837(7)	B–O2	1.398(6)

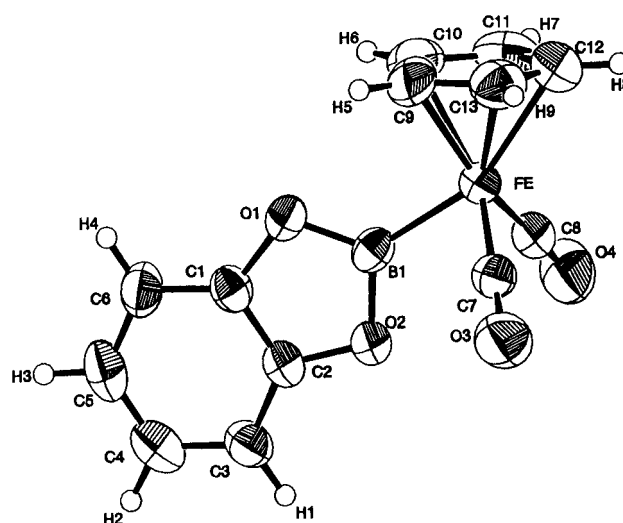
<sup>a</sup> Distances are in angstroms. Estimated standard deviations in the least significant figure are given in parentheses.

**Table 5. Selected Bond Angles for (CO)<sub>5</sub>MnBcat (6)<sup>a</sup>**

	(CO) <sub>5</sub> MnBcat	(CO) <sub>5</sub> MnBcat	(CO) <sub>5</sub> MnBcat
C7–Mn–B	85.5(2)	C11–Mn–B	83.0(3)
C8–Mn–B	178.8(3)	Mn–B–O1	124.3(4)
C9–Mn–B	86.3(3)	Mn–B–O2	125.0(4)
C10–Mn–B	82.1(3)	O1–B–O2	110.7(4)

<sup>a</sup> Angles are in degrees. Estimated standard deviations in the least significant figure are given in parentheses.

**X-ray Crystal Structures for CpFe(CO)<sub>2</sub>Bcat (1), Cp\*Fe(CO)<sub>2</sub>Bcat (2), and (CO)<sub>5</sub>MnBcat (6).** Tables 1–5 provide data collection and refinement parameters and selected bond lengths and angles for compounds **1**, **2**, and **6**. The crystal structure for iron boryl complex **1** has been previously reported in communication form,<sup>21</sup> and an ORTEP diagram is shown in Figure 1. The Fe–B

**Figure 1.** Ortep diagram of CpFe(CO)<sub>2</sub>Bcat (**1**).

bond length was found to be 1.959(6) Å. The difference in dihedral angle between the Cp centroid–Fe–B and O1–B–O2 planes is 7.9°. This structure suggests that a  $\pi$ -interaction may exist between the iron and boron, since the catecholboryl ligand is oriented to allow overlap of the empty boron p-orbital with the CpFe(CO)<sub>2</sub> HOMO.<sup>28,29</sup>

The crystal structure for the Cp\* complex **2** is shown in Figure 2. The Fe–B bond length of 1.980(2) Å is similar to that of the Cp complex **1**. The difference in dihedral angle between the Cp centroid–Fe–B and O1–B–O2 planes is 26.7°, which is significantly larger than that in complex **1**. This larger angle in complex **2** is most likely due to the steric bulk of the pentamethylcyclopentadienyl group that forces the catecholate substituent further out of the Cp centroid–Fe–B plane. This larger angle, coupled with the slight lengthening of the Fe–B bond compared with complex **1**, may indicate a decrease in the  $\pi$ -interaction between the iron and boryl ligand.

The crystal structure for manganese boryl complex **6** has been previously reported<sup>20</sup> and is shown in Figure 3. The Mn–B bond length of 2.108(6) Å is longer than

(28) Schilling, B. E. R.; Hoffmann, R.; Faller, J. W. *J. Am. Chem. Soc.* **1979**, *101*, 592–598.

(29) Schilling, B. E. R.; Hoffmann, R.; Lichtenberger, D. L. *J. Am. Chem. Soc.* **1979**, *101*, 585–591.



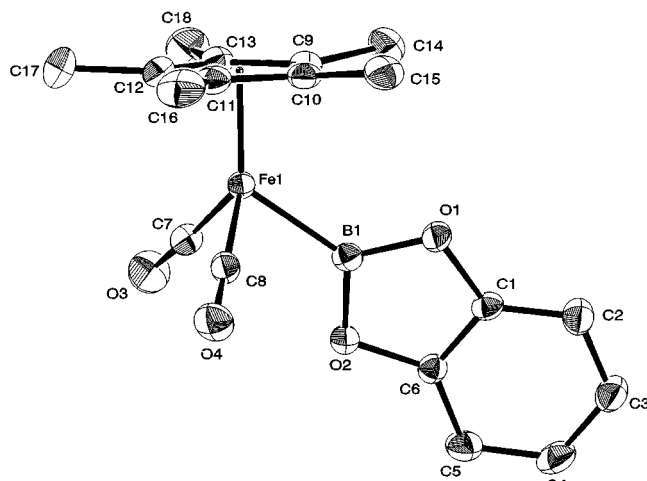


**Figure 2.** Ortep diagram of  $\text{Cp}^*\text{Fe}(\text{CO})_2\text{Bcat}$  (**2**).

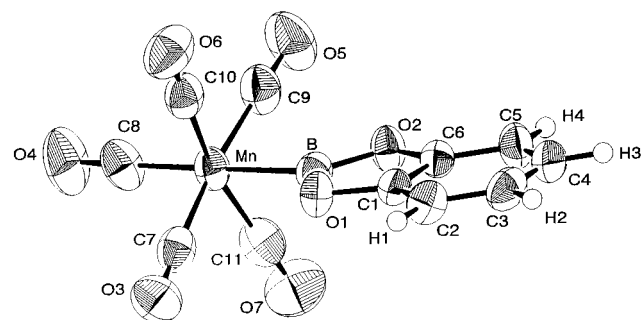
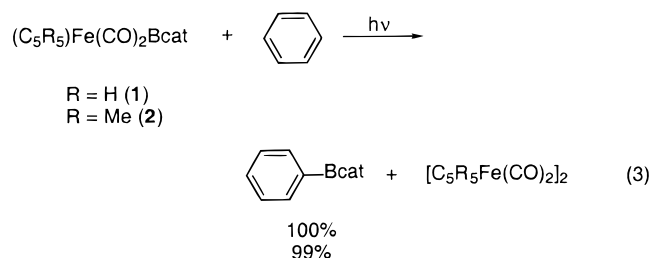


**Figure 3.** Ortep diagram of  $(\text{CO})_5\text{MnBcat}$  (**6**).

the metal–boron distances in other metal carbonyl boryl complexes **1**, **2**, and  $(\text{CO})_4\text{Fe}(\text{Bcat}-t\text{-Bu})_2$  (2.028(7) Å).<sup>30</sup> The Mn–CO bond length trans to the boryl ligand (1.841(6) Å) falls in the range of the other four M–CO distances (1.832(8)–1.870(7) Å). This similarity in M–CO bond distances contrasts the distinct M–CO distances in metal carbonyl complexes of the type  $(\text{CO})_5\text{MR}$  (M = Mn, Re; R = alkyl, H),<sup>31–35</sup> where the M–CO bond length trans to R is shorter than those cis to the R group.

**B. Reaction of Transition-Metal Boryl Complexes with Arenes. Functionalization of Benzene.** Photolysis of iron boryl complex **1** in neat benzene solvent (eq 3) resulted in formation of PhBcat in



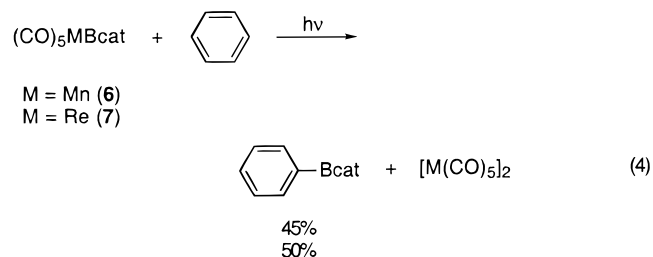
quantitative yield, as determined by  $^1\text{H}$  NMR spectro-

scopy using dodecahydrotriphenylene as an internal standard. The reaction was monitored by  $^{11}\text{B}$  NMR spectroscopy, which showed the formation of a new peak at  $\delta$  32 for the phenylboronate ester product. This product was further characterized by  $^1\text{H}$  NMR spectroscopy and GC/MS. Comparison of these spectral data with those of an independently prepared sample of PhBcat<sup>36</sup> confirmed the identity of the product. The transition-metal product was  $[\text{Cp}^*\text{Fe}(\text{CO})_2]_2$ , as determined by  $^1\text{H}$  NMR and IR spectroscopy. Presumably, the reaction initially produces  $\text{Cp}^*\text{Fe}(\text{CO})_2\text{H}$ , which is known to decompose at room temperature to  $[\text{Cp}^*\text{Fe}(\text{CO})_2]_2$ .<sup>37</sup> Similarly, irradiation of a benzene solution of  $\text{Cp}^*$  iron boryl complex **2** resulted in formation of  $[\text{Cp}^*\text{Fe}(\text{CO})_2]_2$  and PhBcat in 99% yield.

To determine if the  $\text{Cp}^*$  moiety had an effect on the rate of reaction, equimolar solutions of iron complexes **1** and **2** in benzene were irradiated side by side, and the conversion to product was determined qualitatively by  $^{11}\text{B}$  NMR spectroscopy at various times. Reactions of the  $\text{Cp}^*$  complex **2** and of the Cp version **1** displayed equal conversions at various reaction times.

Iron phosphine boryl complexes **3** and **5** also converted solvent benzene to arylboronate esters in high yields. Irradiation of  $\text{CpFe}(\text{PMe}_3)(\text{CO})\text{Bcat}$  (**3**) in benzene- $d_6$  afforded Ph- $d_5$ Bcat in 94% yield. One of the several metal products from photolysis in benzene was determined to be the known hydride  $\text{CpFe}(\text{PMe}_3)(\text{CO})\text{H}$ .<sup>27</sup> The bis(phosphine) complex  $\text{CpFe}(\text{PMe}_3)_2\text{Bcat}$  (**5**) reacted cleanly in benzene- $d_6$  to give Ph- $d_5$ Bcat in 90% yield. The sole metal-containing product from photolysis in benzene was the known hydride  $\text{CpFe}(\text{PMe}_3)_2\text{H}$ .<sup>38</sup>

Photolysis of  $(\text{CO})_5\text{MnBcat}$  (**6**) and  $(\text{CO})_5\text{ReBcat}$  (**7**) resulted in formation of PhBcat in 45% and 50% yields respectively as shown in eq 4. In most cases the



remainder of the boron consisted of multiple products that we have not been able to identify. The transition-metal products of these reactions were  $\text{Mn}_2(\text{CO})_{10}$  or  $\text{Re}_2(\text{CO})_{10}$ , with small amounts of accompanying  $\text{Re}_3(\text{CO})_{12}\text{H}_3$ .<sup>39</sup> These transition-metal products were identified by IR and  $^1\text{H}$  NMR spectroscopy.

**Functionalization of Substituted Arenes.** Reaction of the metal boryl complexes with arene C–H bonds was observed to occur in the presence of accompanying

(35) Masters, A. P.; Richardson, J. F.; Sorensen, T. S. *Can. J. Chem.* **1990**, *68*, 2221–2227.

(36) PhBcat was synthesized by refluxing  $\text{PhB}(\text{OH})_2$  (prepared according to: Bean, F. R.; Johnson, J. R. *J. Am. Chem. Soc.* **1932**, *54*, 4415) and catechol in benzene while azeotropically removing the water with a Dean–Stark apparatus.

(37) Shackleton, T. A.; Mackie, S. C.; Fergusson, S. B.; Johnston, L. J.; Baird, M. C. *Organometallics* **1990**, *9*, 2248–2253.

(38) Green, M. L. H.; Wong, L.-L. *J. Chem. Soc., Dalton Trans.* **1987**, 411–416.

(39) Andrews, M. A.; Kirtley, S. W.; Kaesz, H. D. *Inorg. Synth.* **1977**, *17*, 66.

(30) He, X.; Hartwig, J. F. *Organometallics* **1996**, *15*, 400–407.

(31) Davies, J. A.; El-Ghanam, M.; Pinkerton, A. A. *J. Organomet. Chem.* **1991**, *409*, 367–376.

(32) LaPlaca, S. J.; Hamilton, W. C.; Ibers, J. A.; Davison, A. *Inorg. Chem.* **1969**, *8*, 1928–1935.

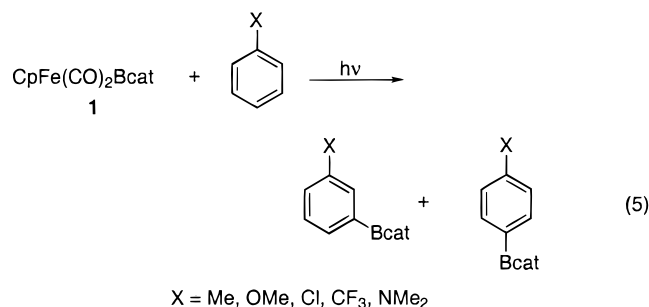
(33) Lee, G.-H.; Peng, S.-M.; Yang, G.-M.; Lush, S.-F.; Liu, R.-S. *Organometallics* **1989**, *8*, 1106–1111.

(34) Lindner, E.; Pabel, M.; Fawzi, R.; Mayer, H. A.; Wurst, K. *J. Organomet. Chem.* **1992**, *435*, 109–121.

**Table 6. Ratio of Product Isomers from Reaction of CpFe(CO)<sub>2</sub>Bcat (1) with C<sub>6</sub>H<sub>5</sub>X**

X	product isomer ratio		
	<i>o</i>	<i>m</i>	<i>p</i>
Me		1.1	1.0
OMe	1.0	1.6	1.1
Cl		1.5	1.0
CF <sub>3</sub>		1.5	1.0
NMe <sub>2</sub>		1.0	8.0

alkyl, trifluoromethyl, chloro, methoxy, and dimethyl-amino groups on the arene, as shown in eq 5. This



chemistry allowed for the evaluation of the electronic interactions involved in the functionalization by using arene substituent effects. Irradiation of CpFe(CO)<sub>2</sub>Bcat (**1**) in a variety of monosubstituted arene solvents led to formation of arylboronate ester products with the ortho, meta, and para ratio of products and yields shown in Table 6. All reactions were monitored by <sup>11</sup>B NMR spectroscopy, which showed a new peak at δ 32–33, indicative of ArBcat products. The different isomers of the various arylboronate ester products were identified by <sup>1</sup>H NMR spectroscopy, GC/MS, and comparison of these spectral data with independently prepared samples.<sup>40</sup> Product ratios and yields were determined by integration of <sup>1</sup>H NMR resonances versus an internal standard of dodecahydrotriphenylene.

Reaction of **1** with substituted arenes resulted in formation of only meta- and para-substituted arylboronate esters for all substrates except anisole, which showed substantial amounts of ortho-substituted product. Irradiation of **1** in *p*-xylene solvent showed very low yields of arylboronate ester product, which is consistent with the lack of ortho products observed in the reactions of most of the monosubstituted arenes. The meta:para ratio of products for all substrates except *N,N*-dimethylaniline and anisole were found to be roughly the same regardless of the substituent. *N,N*-Dimethylaniline showed a preference for reaction at the para position, while anisole formed all three product isomers. The yields of arylboronate esters of the various substituted arenes were determined by either <sup>1</sup>H NMR spectroscopy or GC. The highest yields were obtained for toluene (70%), chlorobenzene (55%), and anisole (52%). The substrates α,α,α-trifluorotoluene and *N,N*-dimethylaniline gave product yields of 33% and 30%, respectively.

Irradiation of rhenium boryl **7** with toluene and α,α,α-trifluorotoluene resulted in only meta- and para-substituted arylboronate esters in roughly the same

**Table 7. Product Ratios from Competition Reactions of CpFe(CO)<sub>2</sub>Bcat (1) with Mixtures of Substituted Arenes**

Substrates		Product Ratio
		1 : 1
		1 : 1
		1 : 3
		1 : 2.4
		1 : 3.4

ratios as those products produced by reaction with **1**. Like iron complex **1**, **7** also formed ortho-substituted products in addition to meta- and para-substituted products upon reaction with anisole. In this case, the major product in the reaction of **7** with anisole was the ortho-substituted arylboronate ester. Overall yields of functionalized product were not measured for **7**.

**Competition Experiments.** To determine the relative rates for reaction of the different substituted arenes with a given metal boryl complex, competition experiments were carried out in which a metal boryl was irradiated in equimolar amounts of two substituted arenes. Ratios of arylboronate ester products shown in Table 7 were determined by GC/MS or <sup>1</sup>H NMR spectroscopy. The product ratios were constant throughout the reaction, suggesting that the products were stable to the reaction conditions and that product ratios were not altered by selective decomposition of products.

Irradiation of **1** with equimolar amounts of toluene and chlorobenzene resulted in roughly 1:1 ratios of tolyl to chlorophenyl boronate esters. A similar product ratio was determined for reactions conducted in the presence of both toluene and α,α,α-trifluorotoluene. *N,N*-Dimethylaniline and anisole were the only two substrates which showed an enhanced rate of reaction over that of toluene. *N,N*-Dimethylaniline reacted 2.4 times faster than toluene, and anisole reacted 3 times faster. Complex **1** was also irradiated with equimolar amounts of *tert*-butylbenzene and *N,N*-dimethylaniline to determine if steric effects of the substituents affected the rate of reaction. *N,N*-Dimethylaniline was found to react about 3.4 times faster than *tert*-butylbenzene. The similarity of this product ratio to that of the reactions involving *N,N*-dimethylaniline and toluene rules out substantial steric effects on the product ratios.

**Measurement of Kinetic Isotope Effects.** Isotope effects of the benzene functionalization reaction were measured in three different ways. First, a competition experiment between benzene and benzene-*d*<sub>6</sub> was conducted by irradiation of the metal boryl complexes **1**, **6**, and **7** in equimolar mixtures of benzene and benzene-*d*<sub>6</sub>. Relative amounts of deuterated and protiated phenylboronate ester products were determined by the ratio of the abundance of the molecular ions in the mass

(40) Morgan, J.; Pinhey, J. T. *J. Chem. Soc., Perkin Trans. 1* **1990**, 715–720.

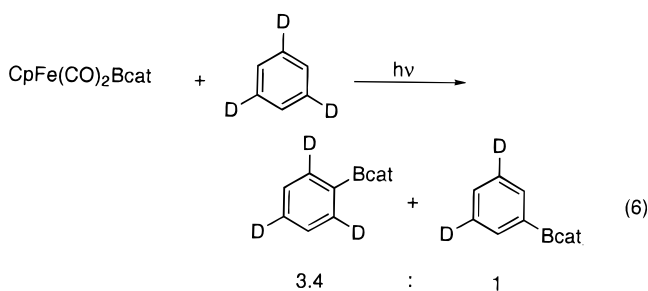
**Table 8. Kinetic Isotope Effects for Photolysis in Benzene/Benzene- $d_6$** 

complex	$k_H/k_D$
CpFe(CO) <sub>2</sub> Bcat ( <b>1</b> )	3.3 ± 0.4
(CO) <sub>5</sub> MnBcat ( <b>6</b> )	2.1 ± 0.1
(CO) <sub>5</sub> ReBcat ( <b>7</b> )	5.4 ± 0.4

spectrum. Kinetic isotope effects  $k_H/k_D$  were found to be 3.3 ± 0.4, 2.1 ± 0.1, and 5.4 ± 0.4, respectively (Table 8).

A second experiment involved a comparison of conversion of complex **1** in benzene and benzene- $d_6$ . Complex **1** in benzene was irradiated side by side with an equally concentrated sample of complex **1** in benzene- $d_6$ . Conversions of the boryl complexes to phenylboronate ester product were qualitatively evaluated at various time points in deuterated and protiated solvents by <sup>11</sup>B NMR spectroscopy. The conversions were found to be indistinguishable at each time.

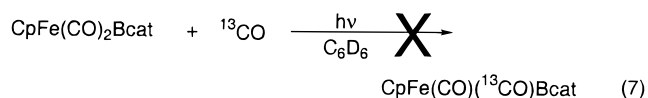
An intramolecular isotope effect was also measured by irradiation of **1** with 10 equiv of 1,3,5-trideuteriobenzene in pentane solvent (eq 6). The ratio of the two



phenylboronate ester products formed from either C–H or C–D cleavage was determined by the relative abundances of the molecular ions in the mass spectrum. This intramolecular isotope effect  $k_H/k_D$  was found to be 3.4, which matches the intermolecular isotope effect observed for reaction of **1** with the mixture of benzene and benzene- $d_6$ .

**Probe for CO Dissociation.** Several experiments were performed to determine whether CO loss is occurring on the reaction pathway, and if so, whether the process is reversible or irreversible. Two samples of **1** in a 25% benzene- $d_6$ /pentane solution were irradiated side by side, one with 5 atm of added CO, and the other without added CO. The relative conversions of the boryl complexes to arylboronate ester products in the presence and absence of CO were evaluated qualitatively by <sup>11</sup>B NMR spectroscopy at various time points. The sample without added CO appeared to react slightly faster than the sample with added CO; however, the difference in conversions was almost immeasurable. This lack of CO inhibition on product formation suggests that CO is either lost irreversibly or not at all.

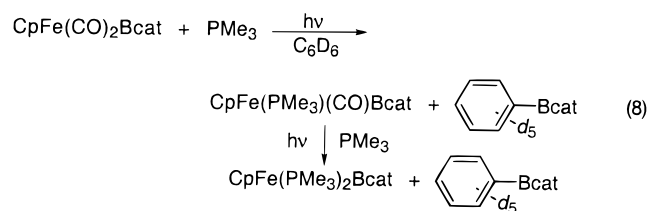
To verify the result of the CO inhibition experiment, a solution of **1** in benzene- $d_6$  was irradiated in the presence of added <sup>13</sup>CO until half of the starting material remained (eq 7). <sup>13</sup>CO was not incorporated



into the starting material, as determined by <sup>13</sup>C NMR

spectroscopy. This result demonstrates that CO is either lost irreversibly or not at all.

To determine if CO dissociation occurs, the photolyses were conducted in the presence of the more soluble and more favorable ligand PMe<sub>3</sub>. A solution of **1** in benzene- $d_6$  was irradiated with 9 equiv of PMe<sub>3</sub> and monitored by <sup>11</sup>B NMR spectroscopy (eq 8). In addition to small



amounts of phenylboronate ester product, a new boryl species was observed by <sup>11</sup>B, <sup>31</sup>P, and <sup>1</sup>H NMR spectroscopy. The identity of this complex was determined to be CpFe(CO)(PMe<sub>3</sub>)Bcat (**3**) by matching the spectral data to those of material prepared independently by the route described in section A on the synthesis of metal boryl complexes. Continued irradiation converted this material into a new complex, which was identified as CpFe(PMe<sub>3</sub>)<sub>2</sub>Bcat (**5**), this time by matching its spectral features to those of a sample prepared by a large-scale photolysis of **1** in the presence of PMe<sub>3</sub>, as described above in section A.

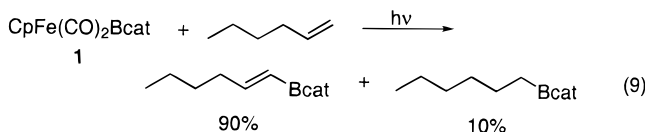
The rate of disappearance of **1** upon photolysis was found to be independent of added phosphine. Two equimolar solutions of **1** in benzene- $d_6$  were irradiated side by side, one with 10 equiv of PMe<sub>3</sub> and one without added PMe<sub>3</sub>. The rate of disappearance of **1** was monitored qualitatively by <sup>11</sup>B NMR spectroscopy and found to be indistinguishable for the two samples over the course of the reaction.

To quantify the effects of added phosphine on PhBcat formation, two equimolar solutions of **1** in benzene- $d_6$  were irradiated side by side in the presence of 5 and 10 equiv of PMe<sub>3</sub>. After conversion of approximately half of the starting material, the reactions were analyzed by <sup>1</sup>H NMR spectroscopy to determine the ratio of phosphine-ligated boryl complex to PhBcat product. The reaction with 10 equiv of PMe<sub>3</sub> gave a 5.7:1 ratio of iron phosphine boryl species to PhBcat, whereas the reaction with 5 equiv of PMe<sub>3</sub> gave a ratio of 2.9:1. Although the metal phosphine species CpFe(CO)(PMe<sub>3</sub>)Bcat (**3**) and CpFe(PMe<sub>3</sub>)<sub>2</sub>Bcat (**5**) react photochemically with benzene to form PhBcat in the absence of phosphine as described above, the presence of free phosphine inhibits this reactivity. Independent experiments showed that complex **3** reacted with phosphine to generate **5** rather than reacting with solvent to generate PhBcat. Moreover, the reaction of **5** toward arene was strongly inhibited by the presence of added phosphine, presumably because of reversible, photochemical ligand dissociation. Thus, the PhBcat measured in the above competition reactions arises only from reactions of the CpFe(CO)<sub>2</sub>Bcat (**1**) starting material.

**C. Reaction of Transition Metal Boryl Complexes with Alkenes. Terminal Alkenes.** The transition-metal boryl complexes described above also react photochemically with alkenes to form vinylboronate esters. Irradiation of **1** with ethylene in alkane solvent produced ethenylBcat as the major product in 88% yield



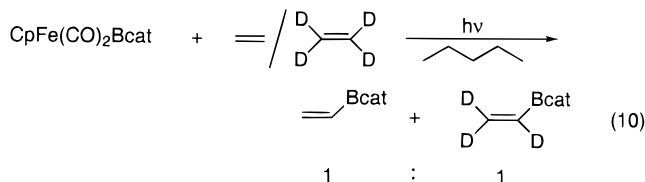
and ethylBcat in 7% yield. As shown in eq 9, irradiation



of **1** dissolved in 1-hexene formed terminal hexenylboronate ester as the major product in 90% yield, in addition to small amounts of hexylboronate ester. These reactions were monitored by  $^{11}\text{B}$  NMR spectroscopy, which showed peaks at  $\delta$  32 and 36, indicative of vinylboronate ester and alkylboronate ester products, respectively. The identity of the products was further confirmed by GC/MS,  $^1\text{H}$  NMR spectroscopy, and comparison of these spectral data with those of independently prepared samples of ethenylBcat, ethylBcat, hexenylBcat, and hexylBcat.<sup>41</sup> The rhenium boryl complex **7** also reacted photochemically with alkenes. Irradiation in neat 1-hexene formed the terminal hexenylboronate ester in 55% yield, as well as hexylboronate ester in 20–25% yield.

**Internal Olefins.** The reaction with internal olefins was not as selective as the reaction with terminal olefins. Irradiation of **7** in neat *trans*-4-octene resulted in vinylboronate ester, at least three isomeric products, and octylboronate ester, as determined by GC/MS. Reaction of cyclohexene led to the formation of cyclohexylboronate ester and one cyclohexenylboronate ester. The  $^{11}\text{B}$  NMR spectrum showed only one peak at  $\delta$  36, indicating that no vinylboronate ester had been formed. Instead, an isomer of the vinylboronate ester product had formed that contains an  $\text{sp}^3$ -carbon–boron bond. This observation was confirmed by the absence of a peak in the GC/MS corresponding to the vinylboronate ester. Irradiation of the rhenium complex with the bicyclic olefin norbornene in pentane provided a single vinylboronate ester product, as well as two norbornylboronate ester products. These products were identified by GC/MS and comparison to a sample of norbornylboronate ester prepared by hydroboration of norbornene.

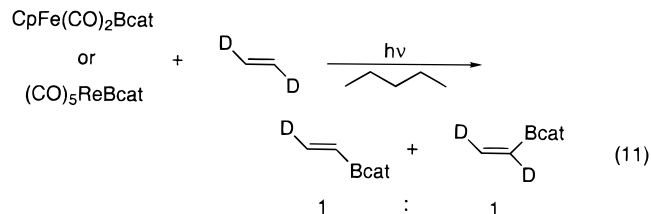
**Measurement of Kinetic Isotope Effects.** Complex **1** in pentane was irradiated with equal volumes of ethylene and ethylene- $d_4$  (eq 10). The reaction was



monitored by  $^{11}\text{B}$  NMR spectroscopy, which showed the formation of vinylboronate ester, with small amounts of alkylboronate ester products as for higher olefins. The ratio of ethenylBcat and ethenylBcat- $d_3$  was determined by the ratio of the abundance of the molecular ions in the mass spectrum. This value of  $k_{\text{H}}/k_{\text{D}}$  was  $1.0 \pm 0.2$ , indicating that there is no intermolecular kinetic isotope effect for this system.

(41) EthylBcat was prepared by  $\text{Rh}(\text{PPh}_3)_3\text{Cl}$ -catalyzed hydroboration of ethylene. EthenylBcat was formed as a minor product of this hydroboration. HexylBcat was prepared by hydroboration of 1-hexene with HBcat. HexenylBcat was prepared by reaction of hexenyllithium with ClBcat.

The intramolecular isotope effect was also determined for iron complex **1** and rhenium boryl complex **7** by irradiation of the metal boryl complexes in pentane with *trans*-1,2-dideuterioethylene (eq 11). The value of  $k_{\text{H}}/$



$k_{\text{D}}$  in this experiment is equal to the ratio of ethenylBcat- $d_2$  to ethenylBcat- $d$ , which was determined by the ratio of the molecular ions in the mass spectrum. In these two systems, there was again no detectable isotope effect.

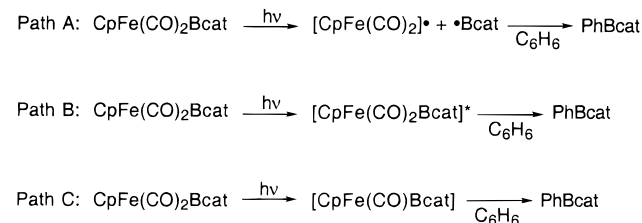
## Discussion

**Mechanism of Arene Functionalization.** Several potential pathways for arene functionalization are shown in Scheme 1. Path A involves formation of a Bcat radical that reacts with arene to give the functionalized product. The Bcat radical would be expected to be electrophilic and may, therefore, react initially with the arene  $\pi$ -system. If the chemistry did occur by attack of a free Bcat radical on free solvent, then one must observe identical isotope effects for all metal boryl systems studied. This free radical would, of course, cleave a C–H or C–D bond with the same selectivity regardless of the origin of the radical. The isotope effects measured for reaction of metal boryl complexes **1**, **6**, and **7** in benzene/benzene- $d_6$  are clearly not equal; thus, a mechanism involving reaction of free Bcat radical with free solvent can be ruled out.

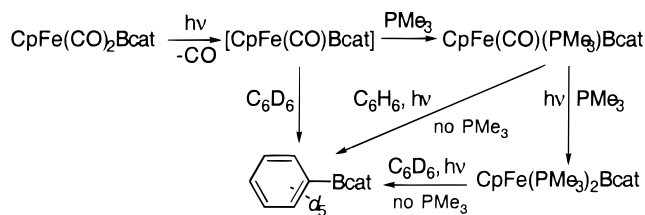
An alternative mechanism would be reaction of a Bcat radical with arene solvent that is coordinated to the metal center. This mechanism seems unreasonable, because coordination of arene to the metal radical would generate a 19-electron species and additional loss of CO would require a two-photon process involving highly reactive intermediates.

Our isotope effect experiments also probed for benzene coordination prior to C–H bond cleavage. If irreversible precoordination occurred, we would expect a small intermolecular isotope effect for reaction with benzene/benzene- $d_6$ , since the  $\eta^2$ -coordination should be similar for benzene and benzene- $d_6$ . In contrast, the intramolecular isotope effect for reaction with 1,3,5-trideuteriobenzene would be large, since the selectivity for reaction with a C–H or C–D bond occurs after the precoordination of arene. Our experiments showed that the inter- and intramolecular isotope effects for  $\text{CpFe}$ -

### Scheme 1



Scheme 2



(CO)<sub>2</sub>Bcat were almost identical (3.3 and 3.4, respectively). Thus, coordination of the arene substrate to the metal center prior to C–H bond cleavage either is fully reversible or does not occur.

Two additional mechanisms involve reaction with either a photochemically generated excited state (path B) or a 16-electron intermediate generated by CO dissociation (path C). Our studies under CO and <sup>13</sup>CO atmospheres showed that added CO does not inhibit the formation of product and that <sup>13</sup>CO is not incorporated into the starting material during the reaction. Neither of these experiments distinguish between the absence of CO dissociation and irreversible dissociation. The reactions conducted in the presence of PMe<sub>3</sub>, however, provide strong evidence for CO dissociation as the initial step of the arene functionalization. The formation of phosphine-ligated boryl complex in competition with arylboronate ester indicates either a common intermediate that reacts with solvent or phosphine (Scheme 2) or separate competitive reactions with PMe<sub>3</sub> and arene solvent. A mechanism involving initial dissociation of CO in competition with direct reaction with phosphine would predict higher conversions of the starting boryl complex as a function of the time of irradiation. Experiments performed with and without added phosphine showed no difference in conversion of **1** at different times, ruling out a separate pathway initiated by reaction with phosphine. In addition, the ratio of metal phosphine boryl complex and arylboronate ester species produced by the photochemical reaction depended on the concentration of phosphine. These data strongly favor a pathway involving photochemical CO dissociation to generate a 16-electron boryl complex that is unusually reactive toward hydrocarbon C–H bonds.

One possible reaction mode for the unsaturated intermediate is an electrophilic aromatic substitution. The boron center in the Bcat moiety, of course, displays some degree of electrophilic character, making an electrophilic aromatic substitution reaction a reasonable pathway for the arene functionalization. Classic electrophilic aromatic substitution reactions show large substituent effects on selectivity for reaction at the different positions of the aromatic ring. If our arene functionalization reactions are occurring through this type of mechanism, then we would expect to observe electronic effects that parallel the directing effects in simple halogenations, nitrations, or Friedel–Crafts alkylations of aromatic systems.

Although the ratios of products in classic electrophilic aromatic substitution chemistry depend on reaction conditions, our results are clearly distinct from standard substituent effects on electrophilic aromatic substitution. For example, the meta:para ratio of products resulting from reaction of the boryl complexes with toluene, chlorobenzene, and α,α,α-trifluorotoluene sub-

strates are virtually identical. Methyl and chloro groups are both ortho,para-directors, whereas the trifluoromethyl substituent is a meta-director. If the reaction were occurring through electrophilic aromatic substitution, we would expect to see arylboronate ester products with *m*-trifluoromethyl, *p*-methyl, and *p*-chloro substituents as the major products. The similarity of the product ratios for varying substituents is strong evidence against an electrophilic aromatic substitution pathway.

The formation of ortho-substituted products with only anisole may be due to an interaction of the oxygen atom with the boryl ligand or transition-metal center, which would lead to C–H bond cleavage at the sterically hindered ortho-position. The ortho-directing ability of the methoxy group is well-established in directed metalation chemistry with alkyllithium reagents.<sup>42</sup> Consistent with coordination of the methoxy group, the less electron rich Re complex provides the ortho-product as the major isomer, whereas the more electron rich Fe complex gives the ortho-isomer as the minor product.

The rate of electrophilic aromatic substitution reactions is also influenced by the electron-donating or -withdrawing ability of the substituent on the aromatic substrate. The rate of substitution should be faster for substrates with activating groups and slower for substrates with deactivating groups. Of our substituents, activating groups include OMe, NMe<sub>2</sub>, Me, and CMe<sub>3</sub>; deactivating groups include Cl and CF<sub>3</sub>. Our competition experiments showed an enhancement in rate of reaction of the reactive intermediate with anisole and *N,N*-dimethylaniline over toluene. Chlorobenzene and trifluorotoluene, however, reacted with this intermediate at nearly the same rate as toluene. An electrophilic aromatic substitution pathway is consistent with the enhanced rate of reaction for substrates with the more donating groups OMe and NMe<sub>2</sub>; however, the magnitude of our effect is much smaller than typically observed for halogenations and nitrations,<sup>43</sup> and the similar rates for reaction of the boryl complexes with Cl- and CF<sub>3</sub>-substituted benzenes are inconsistent with this pathway. These data lead us to rule out the electrophilic aromatic substitution pathway, although the reactive boryl intermediate may have some weak electrophilic character. The small electronic effect on the functionalization process presented here is similar to some previous studies concerning electronic effects on the rate of σ-bond metathesis reactions with substituted arenes<sup>44</sup> and regioselectivity for oxidative addition of toluene by rhodium complexes.<sup>45</sup>

Another possible reaction pathway for the unsaturated intermediate involves an unusual C–H activation process that leads to coupling of the metal-bound covalent ligand with the aryl portion of the substrate. The C–H activation can occur by either (1) oxidative addition of a C–H bond to the unsaturated metal center

(42) Mallan, J. M.; Bebb, R. L. *Chem. Rev.* **1969**, *69*, 693–755.

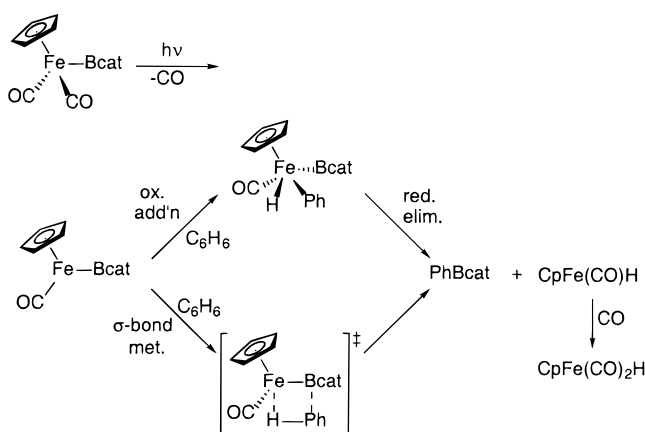
(43) Carey, F. A.; Sundberg, R. J. In *Advanced Organic Chemistry*; Plenum Press: New York, 1990; p 539.

(44) Thompson, M. E.; Baxter, S. M.; Bulls, A. R.; Burger, B. J.; Nolan, M. C.; Santarsiero, B. D.; Schaefer, W. P.; Bercaw, J. E. *J. Am. Chem. Soc.* **1987**, *109*, 203–219.

(45) Jones, W. D.; Feher, F. J. *J. Am. Chem. Soc.* **1984**, *106*, 1650–1663.



Scheme 3



and subsequent reductive elimination of organoborane or (2)  $\sigma$ -bond metathesis (Scheme 3). Oxidative addition is the generally accepted pathway for C–H activation by late-metal systems;<sup>4,5</sup> however, oxidative addition/reductive elimination and  $\sigma$ -bond metathesis mechanisms are difficult to distinguish in the absence of observed aryl hydride intermediates.

**Mechanism of Alkene Functionalization.** The two pathways in Scheme 4 can be envisioned for the functionalization of alkenes. The first pathway involves direct C–H activation of the olefin by the metal center, either by an oxidative addition/reductive elimination sequence or by a concerted  $\sigma$ -bond metathesis mechanism. The second pathway occurs by insertion of the alkene into the metal–boron bond, followed by  $\beta$ -hydrogen elimination to give vinylboronate ester and metal hydride. Both of these mechanisms initially proceed through photochemical loss of CO to form an unsaturated intermediate, which could then coordinate the alkene substrate in an  $\eta^2$ -fashion prior to C–H bond cleavage.

Many mechanisms are possible for formation of the minor alkylboronate ester products. One simple mechanism is metal-catalyzed hydrogenation of the vinylboronate ester. A second involves formation of catecholborane by known hydrogenolysis of the metal boryl complex<sup>20</sup> followed by metal-catalyzed hydroboration of the alkenes.

Our mechanistic information for formation of the major vinylboronate ester products was not clear-cut. Isotope effects for reaction of the metal boryl complex with a mixture of ethylene/ethylene- $d_4$  or with ethylene- $d_2$  could distinguish these paths. If the mechanism occurs through the insertion pathway, we would not expect to see an intermolecular isotope effect for reaction of the metal boryl complex with the ethylene/ethylene- $d_4$  mixture, since protiated and deuterated substrates would have similar rates for insertion into the metal–boron bond. Reaction with ethylene- $d_2$ , however, would be likely to show an intramolecular primary kinetic isotope effect because the metal center could perform either a  $\beta$ -hydrogen or  $\beta$ -deuterium elimination. If the direct C–H activation pathway is followed, we would expect to see both an inter- and intramolecular kinetic isotope effect for reaction of the metal boryl complex

with ethylene/ethylene- $d_4$  and ethylene- $d_2$  if the C–H bond cleavage is irreversible.

Reaction of  $\text{CpFe}(\text{CO})_2\text{Bcat}$  with either ethylene/ethylene- $d_4$  or ethylene- $d_2$  showed no measurable isotope effects. This result was surprising because it is inconsistent with both reaction pathways. One of several explanations could account for the immeasurably small isotope effect. First, the reaction could occur through rate-determining alkene insertion into the metal–boron bond<sup>46–50</sup> and subsequent  $\beta$ -hydrogen elimination of vinylboronate ester. Isotope effects for  $\beta$ -hydrogen elimination are small in some cases.<sup>51–58</sup> Alternatively, a  $\sigma$ -bond metathesis mechanism with an early transition state in which a minimal amount of C–H cleavage has occurred could provide a small isotope effect. Finally a pathway involving the reversible oxidative addition of alkene and subsequent irreversible B–C bond-forming reductive elimination of vinylboronate ester could account for the small  $k_H/k_D$ . In this case, the isotope effect would be generated by only equilibrium and secondary isotope effects.

**Conclusions.** The formation of arylboronate esters from reactions of transition-metal boryl complexes with arenes is unusual for two reasons. First, the process provides functionalized products rather than simply transition-metal aryl complexes. Second, the boryl ligand must alter the properties of the iron, manganese, and rhenium complexes in a fashion that makes them more reactive toward hydrocarbon C–H bonds. One explanation for this enhanced reactivity is that the metal center is more electron rich than it is in more conventional organometallic compounds because of the strong  $\sigma$ -donation by a formally anionic boryl ligand. A second possibility is that the electrophilicity of the boron p-orbital, albeit weak in the case of Bcat ligands, helps to activate the hydrocarbon substrates. Finally, the favorable thermodynamics for formation of B–C bonds<sup>22</sup> may provide a driving force for product formation that is stronger than the driving force for C–C bond formation in conventional systems. These thermodynamic factors may serve to trap a low concentration of C–H activation product that may constantly equilibrate with the starting carbonyl complexes. This hypothesis would predict that C–H activation could be observed with these metal fragments in the form of exchanges between

(47) Westcott, S. A.; Blom, H. P.; Marder, T. B.; Baker, R. T. *J. Am. Chem. Soc.* **1992**, *114*, 8863–8869.

(48) Westcott, S. A.; Marder, T. B.; Baker, R. T. *Organometallics* **1993**, *12*, 975–979.

(49) Burgess, K.; van der Donk, W. A.; Westcott, S. A.; Marder, T. B.; Baker, R. T.; Calabrese, G. C. *J. Am. Chem. Soc.* **1992**, *114*, 9350–9359.

(50) Brown, J. M.; Lloyd-Jones, G. C. *J. Chem. Soc., Chem. Commun.* **1992**, 710–712.

(51) Bullock, R. M. In *Transition Metal Hydrides*; Dedieu, A., Ed.; VCH: New York, 1992; pp 263–307.

(52) McCarthy, T. J.; Nuzzo, R. G.; Whitesides, G. M. *J. Am. Chem. Soc.* **1981**, *103*, 3396–3403.

(53) Ozawa, F.; Ito, T.; Yamamoto, A. *J. Am. Chem. Soc.* **1980**, *102*, 6457–6463.

(54) Komiya, S.; Morimoto, Y.; Yamamoto, A.; Yamamoto, T. *Organometallics* **1982**, *1*, 1528–1536.

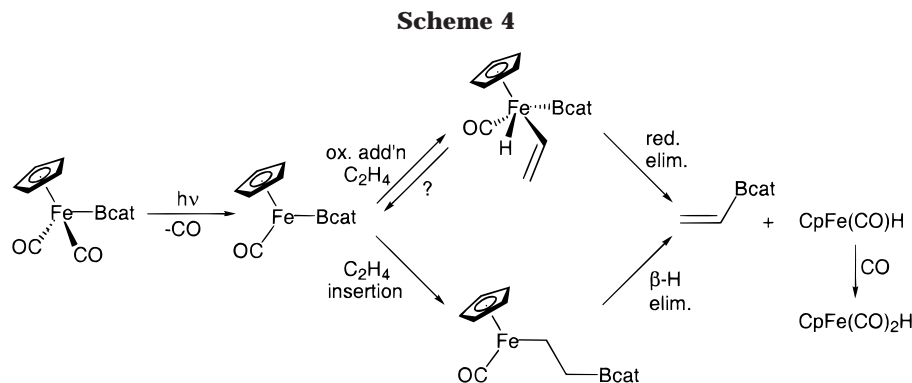
(55) Brainard, R. L.; Whitesides, G. M. *Organometallics* **1985**, *4*, 1550–1557.

(56) Evans, J.; Schwartz, J.; Urquhart, P. W. *J. Organomet. Chem.* **1974**, *81*, C37–C39.

(57) Ikariya, T.; Yamamoto, A. *J. Organomet. Chem.* **1976**, *120*, 257–284.

(58) Burger, B. J.; Thompson, M. E.; Cotter, W. D.; Bercaw, J. E. *J. Am. Chem. Soc.* **1990**, *112*, 1566–1577.

(46) Baker, R. T.; Calabrese, J. C.; Westcott, S. A.; Nguyen, P.; Marder, T. B. *J. Am. Chem. Soc.* **1993**, *115*, 4367–4368.



arenes and Mn, Re, and Fe aryl complexes. Experiments to distinguish between these potential contributions of the boryl ligands to C–H activation are in progress.

### Experimental Section

**General Methods.** Unless otherwise noted, all manipulations were conducted in an inert-atmosphere glovebox or by using standard Schlenk line techniques.  $^1\text{H}$  NMR spectra were recorded on either a General Electric QE-300 or Bruker AM-500 NMR spectrometer, and  $^{11}\text{B}$  and  $^{31}\text{P}\{^1\text{H}\}$  NMR spectra were recorded on an Omega 300 NMR spectrometer.  $^{11}\text{B}$  and  $^{31}\text{P}\{^1\text{H}\}$  chemical shifts are reported in parts per million relative to external standards of  $\text{BF}_3\cdot\text{Et}_2\text{O}$  and 85%  $\text{H}_3\text{PO}_4$ , respectively. Resonances downfield of the standard are assigned positive chemical shifts. Proton chemical shifts are reported in ppm relative to residual protiated solvent as internal standard. Pentane, THF, benzene, and toluene solvents were distilled from sodium/benzophenone ketyl prior to use. Benzene- $d_6$  and anisole were dried over sodium/benzophenone ketyl and degassed before use. Chlorobenzene and  $\alpha,\alpha,\alpha$ -trifluorotoluene were dried over calcium hydride and degassed prior to use. *N,N*-Dimethylaniline was dried over phosphorus pentoxide and distilled prior to use. The metal complexes  $\text{CpFe}(\text{CO})(\text{PMe}_3)\text{H}^{27}$  and  $[\text{Cp}^*\text{Fe}(\text{CO})_2]_2^{59}$  were prepared according to literature procedures. All other chemicals were used as received from commercial suppliers. Photolyses were carried out with a 450 W Hanovia mercury arc lamp in a quartz immersion well using Pyrex reaction vessels placed flush with the immersion well, approximately 0.75 in. from the lamp. Yields were determined by  $^1\text{H}$  NMR through use of internal standards of either trimethoxybenzene or dodecahydrotriphenylene.

**Preparation of  $\text{Na}[\text{Re}(\text{CO})_5]$ ,  $\text{Na}[\text{Mn}(\text{CO})_5]$ ,  $\text{Na}[\text{CpFe}(\text{CO})_2]$ , and  $\text{Na}[\text{Cp}^*\text{Fe}(\text{CO})_2]$  by Na/Hg Reduction.** The appropriate metal dimer was dissolved in THF and reacted with 1% sodium–mercury amalgam (2.5 equiv of Na) for 12 h with vigorous stirring. The solution was removed from the amalgam and filtered through Celite to remove a gray powdery solid. Because the presence of THF led to the decomposition of the metal boryl complexes, it was necessary to remove as much THF from the metal anions as possible. Thorough removal of THF was achieved by first removing the solvent under vacuum to yield a sticky solid, which was ground into a fine powder in the presence of toluene. A suspension of this powder in toluene was heated to 80 °C under vacuum until all the solvent had been removed. This was repeated three times. The resulting solid was washed with toluene to remove dimeric impurities, affording the sodium salt in quantitative yield.

**$\text{CpFe}(\text{CO})_2\text{Bcat}$  (1).** A solution of  $\text{ClBcat}$  (301.8 mg, 1.95 mmol) in 5 mL of toluene was added slowly to a stirred suspension of  $\text{Na}[\text{CpFe}(\text{CO})_2]$  (397.7 mg, 1.99 mmol) in 10 mL of toluene. The reaction was monitored by  $^{11}\text{B}$  NMR spectro-

scopy and stirred for about 1 h until all of the  $\text{ClBcat}$  was consumed. The reaction mixture was filtered through glass wool to remove all solids and the toluene solvent removed under vacuum. The crude product was extracted with pentane and filtered to remove the less soluble dark red impurity,  $[\text{CpFe}(\text{CO})_2]_2$ . Cooling to  $-30$  °C for a very short period of time (less than 20 min) resulted in yellow crystalline product. Crystallization for longer than 20 min resulted in concurrent crystallization of yellow  $\text{CpFe}(\text{CO})_2\text{Bcat}$  with red  $[\text{CpFe}(\text{CO})_2]_2$  impurity. Recrystallization from pentane at  $-30$  °C was necessary to remove traces of boron impurities which resonate at  $\delta$  23 in the  $^{11}\text{B}$  NMR spectrum and are believed to be  $\text{catBOBcat}$ .<sup>60</sup>  $\text{CpFe}(\text{CO})_2\text{Bcat}$  was isolated in 73% yield (419.8 mg).  $^1\text{H}$  NMR ( $\text{C}_6\text{D}_6$ ):  $\delta$  7.13 (m, 2H), 6.81 (m, 2H), 4.20 (s, 5H).  $^{13}\text{C}\{^1\text{H}\}$  NMR ( $\text{C}_6\text{D}_6$ ):  $\delta$  213.96, 150.71, 121.92, 111.48, 83.80.  $^{11}\text{B}$  NMR ( $\text{C}_6\text{D}_6$ ):  $\delta$  51.8. IR (pentane):  $\nu_{\text{CO}}$  2024, 1971  $\text{cm}^{-1}$ . Anal. Calcd for  $\text{C}_{13}\text{H}_9\text{BO}_4\text{Fe}$ : C, 52.77; H, 3.07. Found: C, 52.81; H, 3.14.

**$\text{Cp}^*\text{Fe}(\text{CO})_2\text{Bcat}$  (2).**  $\text{ClBcat}$  (369.3 mg, 2.39 mmol) was reacted with  $\text{Na}[\text{Cp}^*\text{Fe}(\text{CO})_2]$  (677.4 mg, 2.51 mmol) using the same procedure for the synthesis of  $\text{CpFe}(\text{CO})_2\text{Bcat}$  (1). Two recrystallizations from pentane at  $-30$  °C were necessary to remove all traces of red impurity. Additional pure material was obtained from the mother liquor, resulting in a total yield of 71% (620.1 mg) of yellow crystalline product.  $^1\text{H}$  NMR ( $\text{C}_6\text{D}_6$ ):  $\delta$  7.15 (m, 2H), 6.80 (m, 2H), 1.55 (s, 15H).  $^{13}\text{C}\{^1\text{H}\}$  NMR ( $\text{C}_6\text{D}_6$ ):  $\delta$  216.37, 151.43, 122.00, 111.70, 96.07, 10.26.  $^{11}\text{B}$  NMR ( $\text{C}_6\text{D}_6$ ):  $\delta$  54.3. IR (pentane):  $\nu_{\text{CO}}$  1996, 1940  $\text{cm}^{-1}$ . Anal. Calcd for  $\text{C}_{18}\text{H}_{19}\text{BO}_4\text{Fe}$ : C, 59.07; H, 5.23. Found: C, 59.08; H, 5.23.

**$\text{Li}[\text{CpFe}(\text{CO})(\text{PMe}_3)]$  (4).** To a stirred solution of  $\text{CpFe}(\text{CO})(\text{PMe}_3)\text{H}$  (277.0 mg, 1.23 mmol) in pentane was added 0.47 mL of 2.6 M *n*-BuLi (1.22 mmol) in hexane. The solution turned from clear dark yellow to cloudy orange. After the mixture was stirred for 20 min, the orange solid was collected on a fritted funnel and washed several times with pentane, giving the product in 92% yield (261.2 mg).  $^1\text{H}$  NMR ( $\text{C}_6\text{D}_6$ ):  $\delta$  4.51 (s, 5H), 1.47 (d,  $J_{\text{HP}} = 7.4$  Hz, 9H).  $^{31}\text{P}$  NMR ( $\text{C}_6\text{D}_6$ ):  $\delta$  29.3. IR ( $\text{C}_6\text{D}_6$ ):  $\nu_{\text{CO}}$  1915  $\text{cm}^{-1}$ .

**$\text{CpFe}(\text{CO})(\text{PMe}_3)\text{Bcat}$  (3).**  $\text{ClBcat}$  (286.8 mg, 1.86 mmol) was reacted with  $\text{Li}[\text{CpFe}(\text{CO})(\text{PMe}_3)]$  (430.6 mg, 1.86 mmol) using the same procedure for the synthesis of  $\text{CpFe}(\text{CO})_2\text{Bcat}$  (1). Crystallization from pentane at  $-30$  °C afforded a powder containing both black and yellow solids. Only one compound was observed by NMR spectroscopy. The yellow material was separated by sublimation (65 °C, 0.01 mmHg) and subsequent recrystallization from pentane to give pale yellow crystalline material in 33% yield (210.2 mg).  $^1\text{H}$  NMR ( $\text{C}_6\text{D}_6$ ):  $\delta$  7.18 (m, 2H), 6.84 (m, 2H), 4.31 (d,  $J_{\text{HP}} = 1.5$  Hz, 5H), 0.92 (d,  $J_{\text{HP}} = 9.4$  Hz, 9H).  $^{13}\text{C}\{^1\text{H}\}$  NMR ( $\text{C}_6\text{D}_6$ ):  $\delta$  219.17 (d,  $J_{\text{CP}} = 28.6$  Hz), 151.47, 121.54, 111.24, 81.77, 22.18 (d,  $J_{\text{CP}} = 30.5$  Hz).  $^{11}\text{B}$

(60) Clegg, W.; Lawlor, F. J.; Marder, T. B.; Nguyen, P.; Norman, N. C.; Orpen, A. G.; Quayle, M. J.; Rice, C. R.; Robins, E. G.; Scott, A. J.; Souza, F. E. S.; Stringer, G.; Whittell, G. R. *J. Chem. Soc., Dalton Trans.* **1998**, 301–309.

(59) Catheline, D.; Astruc, D. *Organometallics* **1984**, *3*, 1094–1100.

NMR ( $C_6D_6$ ):  $\delta$  57.5.  $^{31}P\{^1H\}$  NMR ( $C_6D_6$ ):  $\delta$  39.2. IR ( $C_6D_6$ ):  $\nu_{CO}$  1927  $cm^{-1}$ . Anal. Calcd for  $C_{15}H_{18}BO_3PFe$ : C, 52.38; H, 5.28. Found: C, 52.57; H, 5.37.

**CpFe(PMe<sub>3</sub>)<sub>2</sub>Bcat (5).** PMe<sub>3</sub> (5 equiv) was transferred by vacuum techniques into a solution of CpFe(CO)<sub>2</sub>Bcat (**1**; 416.8 mg, 1.41 mmol) in 30 mL of pentane in a glass bomb equipped with a stir bar. This yellow solution was irradiated with stirring for at least 6 h. The reaction was monitored by  $^{11}B$  NMR spectroscopy until all of the monosubstituted product, CpFe(CO)(PMe<sub>3</sub>)Bcat (**3**) at  $\delta$  57, was converted to the disubstituted product at  $\delta$  60. When the reaction was complete, all volatile materials were removed under vacuum, and the residue was extracted with pentane. The extracts were filtered through glass wool, condensed, and crystallized at  $-30^\circ C$  to yield dark yellow-amber crystals. Further crystallization from toluene was necessary to remove all traces of monosubstituted product impurity, affording the bis(phosphine) complex **5** in 52% yield (286.7 mg). An additional 24% (132.3 mg) of product in roughly 95% purity was obtained from the toluene mother liquor.  $^1H$  NMR ( $C_6D_6$ ):  $\delta$  7.19 (m, 2H), 6.86 (m, 2H), 4.14 (t,  $J_{HP} = 1.7$  Hz, 5H), 1.05 (vt, 18H).  $^{13}C\{^1H\}$  NMR ( $C_6D_6$ ):  $\delta$  151.91, 120.80, 110.54, 78.09, 24.72 (vt).  $^{11}B$  NMR ( $C_6D_6$ ):  $\delta$  60.  $^{31}P\{^1H\}$  NMR ( $C_6D_6$ ):  $\delta$  38.0. Anal. Calcd for  $C_{17}H_{27}BO_2P_2Fe$ : C, 52.09; H, 6.94. Found: C, 52.40; H, 6.75.

**(CO)<sub>5</sub>MnBcat (6).** ClBcat (208.8 mg, 1.35 mmol) was reacted with Na[Mn(CO)<sub>5</sub>] (294.5 mg, 1.35 mmol) using the same procedure for the synthesis of CpFe(CO)<sub>2</sub>Bcat (**1**). After initial filtration of solid, the resulting yellow toluene solution was condensed, layered with pentane, and cooled to  $-30^\circ C$ , affording square colorless crystals. Additional material was obtained from the mother liquor to give an overall yield of 77% (327.0 mg).  $^1H$  NMR ( $C_7D_8$ ):  $\delta$  6.97 (m, 2H), 6.74 (m, 2H).  $^{13}C\{^1H\}$  NMR ( $C_6D_6$ ):  $\delta$  210.68, 209.62, 150.34, 122.86, 112.29.  $^{11}B$  NMR ( $C_6H_6$ ):  $\delta$  49. IR (Nujol):  $\nu_{CO}$  2112 (w), 2009 (v. broad, vs)  $cm^{-1}$ . Anal. Calcd for  $C_{11}H_4BO_7Mn$ : C, 42.09; H, 1.28. Found: C, 41.80; H, 1.38.

**(CO)<sub>5</sub>ReBcat (7).** ClBcat (325.9 mg, 2.11 mmol) was reacted with Na[Re(CO)<sub>5</sub>] (737.6 mg, 2.11 mmol) using the same procedure for synthesis of CpFe(CO)<sub>2</sub>Bcat (**1**). After initial filtration of solid, the yellow toluene solution was condensed, layered with pentane, and cooled to  $-30^\circ C$ . The resulting white crystals were recrystallized two more times from pentane to give analytically pure material in 30% yield (277.4 mg).  $^1H$  NMR ( $C_6D_6$ ):  $\delta$  7.09 (m, 2H), 6.77 (m, 2H).  $^{13}C\{^1H\}$  NMR ( $C_6D_6$ ):  $\delta$  183.58, 182.21, 150.48, 122.76, 112.34.  $^{11}B$  NMR ( $C_6D_6$ ):  $\delta$  44. IR ( $C_6D_6$ ):  $\nu_{CO}$  2129, 2051, 2016 (vs)  $cm^{-1}$ . Anal. Calcd for  $C_{11}H_4BO_7Re$ : C, 29.68; H, 0.91. Found: C, 29.75; H, 0.92.

**General Procedure for Photochemical Reaction of Metal Boryls with Arene/Alkene Substrates.** The metal boryl complex (5 mg) was dissolved in 0.5 mL of neat substrate and the solution transferred to an NMR tube. For the ethylene substrate, the metal boryl complex (5 mg) was dissolved in 0.5 mL of pentane and transferred to a thick-walled NMR tube, and 100 equiv of ethylene was condensed into the tube, which was then flame-sealed.  $^{11}B$  NMR spectra were recorded for the starting material. The sample was irradiated with periodic monitoring of the reaction by  $^{11}B$  NMR spectroscopy.

**Isotope Effect Measurements. (a) Arene Substrate.** The metal boryl complex (5 mg) was added to an NMR sample tube as a solid. Equimolar amounts of benzene (0.30 mL) and benzene-*d*<sub>6</sub> (0.30 mL) were added to the tube by syringe, and the tube was capped with a septum. The sample was irradiated until all starting material was consumed as determined by  $^{11}B$  NMR spectroscopy. The solution inside the tube was analyzed by GC/MS to determine the ratio of protiated and deuterated

phenylboronate esters by the abundance of their molecular ions, which is a direct measurement of the kinetic isotope effect,  $k_H/k_D$ . A similar procedure was used to determine the intramolecular isotope effect for reaction with 1,3,5-trideuteriobenzene.

**(b) Alkene Substrate.** The metal boryl complex (5 mg) was dissolved in pentane (0.5 mL) and transferred to an NMR tube. *trans*-1,2-Dideuterioethylene (20 equiv) was condensed into the tube using vacuum techniques, and the tube was flame-sealed. The solution was irradiated and monitored by  $^{11}B$  NMR spectroscopy until the starting material was completely consumed. The products were analyzed by GC/MS, and the value for the kinetic isotope effect was determined by the ratio of the abundance of the molecular ions of ethenyl-*d*<sub>2</sub>-Bcat and ethenyl-*d*-Bcat. A similar procedure was used for reaction of the metal boryl with equal amounts of ethylene and ethylene-*d*<sub>4</sub>.

**Competition Experiments.** The metal boryl complex was added to an NMR tube as a solid. Equimolar amounts of substituted arene were added into the NMR tube by syringe, and the tube was capped with either a septum or screw cap. The solution was irradiated until all the starting material was consumed, as determined by  $^{11}B$  NMR spectroscopy. The solution was then analyzed by GC/MS to determine the relative ratio of arylboronate ester products derived from the two substrates.

**CO Inhibition Experiment.** The metal boryl complex (10 mg) was dissolved in pentane (0.6 mL). Benzene was added to this solution (0.2 mL) by syringe, and the solution was then added to two NMR tubes (0.4 mL in each). Carbon monoxide (5 atm) was introduced into one of the tubes.  $^{11}B$  NMR spectra of the two samples were recorded before irradiation side by side. During the course of irradiation,  $^{11}B$  NMR spectra were periodically recorded of both samples, and the amount of product was qualitatively evaluated at each time point.

**$^{13}CO$  Experiment.** Iron boryl complex **1** (6 mg) was dissolved in  $C_6D_6$  and transferred to a Young NMR tube.  $^{13}CO$  (1.8 atm) was introduced into the tube.  $^{11}B$ ,  $^1H$ , and  $^{13}C$  NMR spectra were recorded for the starting material. The solution was irradiated until roughly half the starting material remained by  $^{11}B$  NMR spectroscopy.  $^{13}C$  NMR spectroscopy of this sample showed no incorporation of the labeled CO into the starting material.

**PMe<sub>3</sub> Trapping Experiment.** Iron boryl complex **1** (5 mg) was dissolved in benzene-*d*<sub>6</sub> (0.5 mL) and transferred to an NMR sample tube. PMe<sub>3</sub> (9 equiv) was condensed into the tube using vacuum techniques, and the tube was flame-sealed.  $^{11}B$ ,  $^{31}P$ , and  $^1H$  NMR spectra were recorded of the starting material. The solution was irradiated and periodically monitored by  $^{11}B$ ,  $^{31}P$ , and  $^1H$  NMR spectroscopy.

**Acknowledgment.** We gratefully acknowledge support from the National Science Foundation (CHE-9617171), a Camille Dreyfus Teacher/Scholar Award, and a National Science Foundation Young Investigator Award. J.F.H. is a fellow of the Alfred P. Sloan Foundation.

**Supporting Information Available:** Tables of crystal data, structure solution and refinement, positional parameters, bond lengths and angles, torsion angles, Cartesian coordinates, and anisotropic thermal parameters for Cp\*Fe(CO)<sub>2</sub>Bcat (**2**). This material is available free of charge via the Internet at <http://pubs.acs.org>.

OM990113V